

Cold Molecule Spectroscopy for Constraining the Evolution of the Fine Structure Constant

Eric R. Hudson,* H. J. Lewandowski, Brian C. Sawyer, and Jun Ye†

*JILA, National Institute of Standards and Technology and University of Colorado, Boulder, Colorado 80309-0440, USA
and Department of Physics, University of Colorado, Boulder, Colorado 80309-0440, USA*

(Received 9 January 2006; published 14 April 2006)

We report precise measurements of ground-state, Λ -doublet microwave transitions in the hydroxyl radical molecule (OH). Utilizing slow, cold molecules produced by a Stark decelerator we have improved over the precision of the previous best measurement 25-fold for the $F' = 2 \rightarrow F = 2$ transition, yielding $(1\,667\,358\,996 \pm 4)$ Hz, and by tenfold for the $F' = 1 \rightarrow F = 1$ transition, yielding $(1\,665\,401\,803 \pm 12)$ Hz. Comparing these laboratory frequencies to those from OH megamasers in interstellar space will allow a sensitivity of 1 ppm for $\Delta\alpha/\alpha$ over $\sim 10^{10}$ yr.

DOI: 10.1103/PhysRevLett.96.143004

PACS numbers: 33.20.Bx, 33.15.Pw, 33.55.Be, 39.10.+j

Current theories that attempt to unify gravity with the other fundamental forces predict spatial and temporal variations in the fundamental constants, including the fine structure constant, α [1]. Compellingly, a space-time varying coupling constant, such as α , implies violation of both Lorentz invariance and *CPT* symmetry [2]. Comparison of different atomic clock systems [3] has provided tight constraints on the time variation of various fundamental constants, including α , during the modern epoch. However, observation of absorption lines in distant quasars [4,5] provides conflicting results about possible α variation over cosmological time. Since the largest α variation may have occurred during the early Universe [6], the inconsistent conclusions of the quasar measurements are most interesting. Because of the use of spatially diverse absorbers, these measurements are sensitive to relative Doppler shifts, and therefore an independent confirmation of the variation of α is important.

Recently, there has been much interest in using OH megamasers in interstellar space to constrain the evolution of fundamental constants [7–9] with several key advantages. Most importantly, the multiple lines (that have different dependence on the fundamental constants) arising from one of these localized sources differentiate the relative Doppler shift from true variation in the transition frequency. Furthermore, it has been shown that the sum and difference of the $\Delta F = 0$ (F is total angular momentum) transition frequencies in the ground Λ doublet of OH depend on α as $\alpha^{0.4}$ and α^4 , respectively (see Fig. 1) [7]. Thus, by comparing these quantities as measured from OH megamasers to laboratory values and assuming α variation dominates over other fundamental constants, it is possible to remove the Doppler shift systematic and constrain α over cosmological time. Furthermore, because of the unique properties of the Λ doublet, the $\Delta F = 0$ transitions are extremely insensitive to magnetic fields. However, as pointed out by Darling [7], for the current limits on $\Delta\alpha/\alpha$ the change in the relevant measurable quantities is on the order of 100 Hz, which, prior to this work, was the accuracy of the best laboratory based measurement [10]. Moreover, an astrophysical measurement of OH megamas-

ers, scheduled for later this year, expects a precision better than 100 Hz [11], and thus better laboratory measurements of the OH Λ -doublet microwave transitions are imminently needed to allow for tighter constraints on $\Delta\alpha/\alpha$.

Despite the prominence of the OH radical in molecular physics, the previous best measurement of the OH ground Λ doublet has stood for over 30 years [10]. This lack of improvement was due to the relatively slow progress in the center-of-mass motion control of molecules, which limited the maximum interrogation time, and thus the spectroscopic resolution. The ability of a Stark decelerator [12,13] to provide slow, cold pulses of molecules makes it an ideal source for molecular spectroscopy [14]. In this

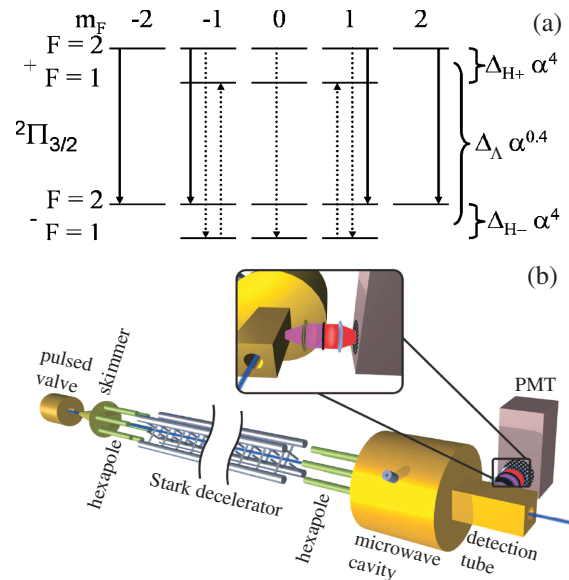


FIG. 1 (color online). (a) OH ground Λ -doublet state. The arrows represent the effect of the applied microwave pulses for the $2 \rightarrow 2$ (solid arrows) and $1 \rightarrow 1$ (dotted arrows) transitions. The α dependence of the spacings is denoted by curly brackets, where $\Delta_{H+} = 19.440\,706(50) \times 10^9$ MHz, $\Delta_{\Lambda} = 11.926\,362\,834(13)$ GHz, and $\Delta_{H-} = 18.750\,512(50) \times 10^9$ MHz. (b) Schematic of experiment (inset depicts detection region).

work, a Stark decelerator is used along with standard microwave spectroscopy techniques to perform the best measurement to date of the $\Delta F = 0$, Λ -doublet microwave transitions in OH, which with appropriate astrophysical measurements can be used to constrain $\Delta\alpha/\alpha$ with a sensitivity of 1 ppm over the last $\sim 10^{10}$ yr.

In its ro-vibronic ground state OH is a Hund's case (a) molecule with a $^2\Pi$ configuration and total molecule-fixed angular momentum of $\Omega = \frac{3}{2}$. For the most abundant isotopomer ($O^{16}H$), the oxygen has no nuclear spin and the hydrogen carries a nuclear spin of $\frac{1}{2}$ leading to two total spin states with $F = 1$ and 2. Because the unpaired electron in OH has one unit of orbital angular momentum, these ro-vibronic ground states are " Λ doubled," leading to the closely spaced, opposite-parity, Λ -doublet states shown in Fig. 1(a) labeled as $|F, m_F, \text{parity}\rangle$. Though molecules are decelerated only in the $|2, \pm 2, +\rangle$ and $|2, \pm 1, +\rangle$ states, the field-free region from the hexapole to the microwave cavity leads to an equal redistribution of the population among the five magnetic sublevels of the $F = 2$ upper doublet state. In this work, both $\Delta F = 0$ electric dipole transitions between the upper and lower doublet states are studied. Though these transitions exhibit large Stark shifts (as is necessary for Stark deceleration), they show remarkably small Zeeman shifts. In fact, because the magnetic dipole operator respects parity, one expects the $\Delta F = 0$ transitions of a pure case (a) molecule to show no magnetic field dependence. Nonetheless, because the hyperfine splitting differs in the upper and lower doublet, and part of the $|m_F| = 1$ magnetic dipole moment comes from mixing with the other hyperfine component, there is a small quadratic shift of the $|2, \pm 1, +\rangle \rightarrow |2, \pm 1, -\rangle$ transition frequency (150 Hz/Gauss²). Furthermore, because OH is not completely case (a) (i.e., the electron's orbital angular momentum and spin are slightly decoupled from the axis), the g factor is slightly larger in the lower doublet [15]. Thus, transitions between the $m_F < 0$ ($m_F > 0$) components are blueshifted (redshifted) relative to the zero field value. Hence, for experiments probing both positive and negative m_F components such as this work, the g -factor difference leads to a broadening and eventually a bifurcation in the line shape for increasing magnetic field. This effect, explored at relatively large fields (0.6–0.9 T), was found to shift the $\Delta F = 0$ transition frequencies of the $|2, \pm 2, +\rangle$, $|2, -1, +\rangle$, and $|1, 1, +\rangle$ states at a rate of $-\text{sgn}(m_F) \times 2.7$ kHz/Gauss, and the $|1, -1, +\rangle$ and $|2, 1, +\rangle$ states at a rate of $-\text{sgn}(m_F) \times 0.9$ kHz/Gauss [15]. For even population distribution this effect leads to a shift of 450 Hz/Gauss and -900 Hz/Gauss for the $2 \rightarrow 2$ and $1 \rightarrow 1$ transitions, respectively.

Shown in Fig. 1(b) is a schematic of our experimental setup. OH molecules seeded in Xenon are created in a pulsed discharge [16], producing a molecular pulse with a mean speed of 410 m/s and 10% longitudinal velocity spread. Following a skimmer is an electrostatic hexapole

used to couple the molecules into our Stark decelerator transversely [13,17,18]. The Stark decelerator is used in a variety of operating conditions, yielding pulses of molecules at a density of 10^6 cm⁻³ with mean speeds chosen between 410 m/s and 50 m/s with longitudinal temperatures between 1 K and 5 mK, respectively. The present density of the OH beam limits any density related frequency shift to below 1 mHz. Once the molecular pulse exits the decelerator it is focused by a second hexapole to the detection region. Located between the second hexapole and the detection region is a 10 cm long cylindrical microwave cavity with its axis aligned to the molecular beam. The microwave cavity is operated near the TM_{010} mode, such that the electric field is uniform over the region sampled by the molecules. The microwave cavity is surrounded by highly magnetically permeable material to provide shielding from stray magnetic fields. From measurements of the magnetically sensitive $F = 2 \rightarrow F = 1$ transition frequency the residual field in the cavity was determined to be < 2 milliGauss. This small field results in an absolute Zeeman shift of < 0.9 Hz and < 1.8 Hz for the $2 \rightarrow 2$ and $1 \rightarrow 1$ transitions, respectively. Note that this is a cautious upper bound on the Zeeman shift, since it is based on work performed at ~ 1 T magnetic field, where the angular momentum decoupling is enhanced. Furthermore, the use of all metal microwave cavity at the interaction region has removed all electric field related frequency shifts, as an applied external field as large as 700 V/cm resulted in no detectable shift in the measured transition frequencies.

Two independently switchable microwave synthesizers, both referenced to the Cesium standard, are used to provide the microwave radiation for driving the Λ -doublet transitions. For probing the $|2, m_F, +\rangle \rightarrow |2, m_F, -\rangle$ Λ -doublet transition ($2 \rightarrow 2$) only one synthesizer is needed since the molecules enter the cavity in the $F = 2$ state. Accordingly, two synthesizers are needed for probing the $1 \rightarrow 1$ transition. The first synthesizer's field transfers molecules from the $F = 2$ upper doublet state to the $F = 1$ lower doublet state. The second synthesizer's field then probes the $1 \rightarrow 1$ transition. After the molecules exit the cavity, the population of the upper doublet is probed by laser-induced fluo-

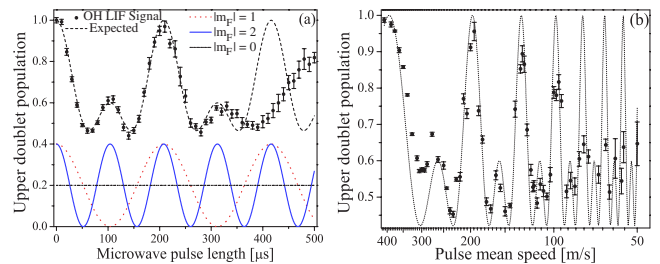


FIG. 2 (color online). (a) Rabi-flopping as a function of time. The contributions of the individual magnetic sublevels are shown near the bottom, while the sum is shown as the dashed line. (b) Rabi-flopping as a function of velocity for a fixed (spatial) length microwave pulse. The dashed line is the expected result.

rescence (LIF). For the LIF measurement, the molecules are excited along the $^2\Sigma_{1/2}(v=1) \leftarrow ^2\Pi_{3/2}(v=0)$ line at 282 nm by light produced from a doubled pulsed-dye laser. This excited state decays primarily along $^2\Sigma_{1/2}(v=1) \rightarrow ^2\Pi_{3/2}(v=1)$ at 313 nm. The redshifted fluorescence is collected and imaged onto a photomultiplier tube coupled to a photon counter.

To characterize the performance of the microwave cavity, the population in the upper doublet was recorded as a function of applied microwave pulse length as shown in Fig. 2(a) (so-called Rabi flopping). For the data shown, the molecules were decelerated to 200 m/s and a microwave pulse resonant with the $2 \rightarrow 2$ transition was applied such that its midpoint time coincided with the molecules being at the cavity center. Thus, as the pulse length was increased the molecules encountered a pulse that grew symmetrically about the cavity center. Because the LIF detection scheme is sensitive to all molecules in the upper doublet, and the applied microwave field simultaneously drives transitions between the different magnetic sublevels, the Rabi-flopping signal is more complicated than the traditional $\sin^2(\frac{\omega'_R t_p}{2})$. Here ω'_R is the effective Rabi frequency given in terms of the detuning, δ , and Rabi frequency, ω_R , as $\omega'_R = \sqrt{\delta^2 + \omega_R^2}$, and t_p is the microwave pulse length. As shown in Fig. 1(a) for the $2 \rightarrow 2$ transition (solid arrows), both the $|m_F| = 2$ and $|m_F| = 1$ magnetic sublevels are driven by the microwave field (the $|m_F| = 0$ level has a zero transition moment). Because the electric dipole transition moment of the $|m_F| = 2$ is twice that of $|m_F| = 1$ [19], the Rabi-flopping signal exhibits beating. The calculated individual magnetic sublevel contributions are shown at the bottom of Fig. 2(a) with their sum represented by the dashed line plotted over the data. The data points were determined by comparing the populations in the upper doublet at the detection region with and without the microwave field applied. Clearly, the behavior is as expected until $t_p \geq 300 \mu\text{s}$ when ω_R of both the $|m_F| = 2$ and $|m_F| = 1$ transitions appears to decrease. This reduction in ω_R is the result of the electric field diminishing near the cavity end caps [20].

Alternatively to fixing the molecular velocity v and varying t_p , the Stark decelerator allows v to be varied while applying a fixed (spatial) length microwave pulse. This allows a check of systematics associated with beam velocity. Data taken in this manner are shown in Fig. 2(b), where a microwave pulse resonant with the $2 \rightarrow 2$ transition was applied for the entire time the molecules were in the cavity. The microwave power for this measurement was chosen such that molecules with a 400 m/s velocity underwent one complete population oscillation (i.e., a 2π pulse for the $|m_F| = 1$ and a 4π pulse for the $|m_F| = 2$ transitions). This was done so that population revivals occurred at velocities that were integer submultiples of 400 m/s. While the behavior agrees well with the expected (dotted line), there are two noticeable deviations. First, for

$270 \text{ m/s} \leq v \leq 400 \text{ m/s}$ the fringe visibility is less than expected. This is because molecules with these relatively high velocities have not been decelerated out of the background molecular pulse. Thus, molecules with a large distribution of speeds (as compared to the decelerated molecules) are detected, leading to reduced contrast. Second, substantial decoherence is observed for $v \leq 130 \text{ m/s}$. This decoherence was experimentally determined to be the result of microwave radiation being reflected off the decelerator back into the cavity. Because this decoherence is due to reflected radiation it is microwave power dependent, and presents no problem for the transitions frequency measurements, which use $<10\%$ of the microwave power used in Fig. 2, such that no noticeable decoherence occurs.

Because two magnetic sublevels with differing ω_R 's undergo the $2 \rightarrow 2$ transition, the traditional Rabi-spectroscopy method of applying a π pulse over the length of the cavity is not optimal. Thus, for measurements of the $2 \rightarrow 2$ transition frequency, the microwave power was chosen such that for $\delta = 0$ the maximum contrast was produced with as small a microwave power as possible [i.e., transfer the molecules to the first dip in Fig. 2(a) over the length of the cavity]. Representative data for the $2 \rightarrow 2$ transition is shown in Fig. 3(a), where the driving frequency f is varied under a fixed microwave power. Data points in this graph were generated by comparing the population in the upper doublet at the detection region with and without the probing microwave field. The fit to the data (solid line) is generated from the typical Rabi line shape formula except contributions from the different magnetic sublevels are included. For probing the $1 \rightarrow 1$ transition it is necessary to prepare the molecules in a $F = 1$ level since they originate in the $|2, m_F, +\rangle$ level from the Stark decelerator. This is accomplished by using the first $70 \mu\text{s}$ the molecules spend in the cavity to drive them on the satellite $2 \rightarrow 1$ line, yielding molecules in the $|1, \pm 1, -\rangle$ and $|1, 0, -\rangle$ states (downward dotted arrows in Fig. 1). The remaining time the molecules spend in the cavity (depending on v) is then used to probe the $1 \rightarrow 1$ transition frequency by applying a π pulse, which transfers only the $|m_F| = 1$ molecules to the upper doublet (upward dotted arrows in Fig. 1). Representative data for the $1 \rightarrow 1$ transition is shown in Fig. 3(b). In contrast to the $2 \rightarrow 2$

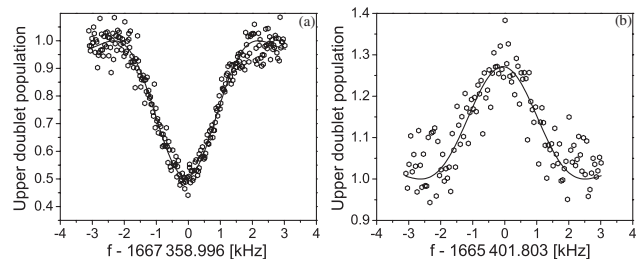


FIG. 3. Representative line shape of the $2 \rightarrow 2$ (a) and $1 \rightarrow 1$ (b) transitions. Both measurements correspond to an interaction time of 0.5 ms ($v = 200 \text{ m/s}$). A center frequency is extracted from each fit (solid line).

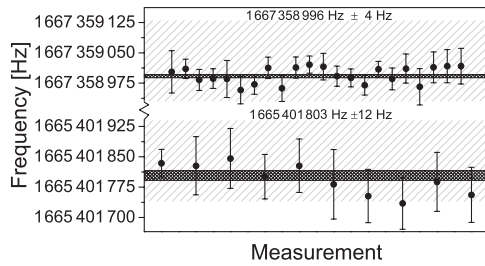


FIG. 4. Results of multiple measurements of the $2 \rightarrow 2$ transition (upper) and the $1 \rightarrow 1$ transition (lower).

line, the LIF signal is maximum on resonance because molecules are being transferred into the detected upper doublet. Also, because only 40% of the population participate in the transitions (i.e., the $|m_F| = 1$) the contrast between on and off resonance is reduced relative to the $2 \rightarrow 2$ transition, leading to a slightly larger error for determining the center frequency. For both panels of Fig. 3 the molecules were decelerated to 200 m/s yielding linewidths of 2 kHz. A typical fit determines the center frequency within 20 to 50 Hz, depending on the transition.

The results of several measurements of both the $2 \rightarrow 2$ and $1 \rightarrow 1$ center frequencies are displayed in Fig. 4. Each point and its error bar represent the result of a fit to a measured line shape like those shown in Fig. 3. Using the standard error of each fit as a weight, the mean and standard error of the transition frequencies are found to be $(1\,667\,358\,996 \pm 4)$ Hz and $(1\,665\,401\,803 \pm 12)$ Hz for the $2 \rightarrow 2$ and $1 \rightarrow 1$, respectively. For comparison, the lightly hatched boxes represent the bounds set on the transition frequency by the previous best measurement [10], while the limits produced by this measurement are displayed as darker cross-hatched boxes. The transition frequencies reported here are limited only by statistical uncertainties, as we estimate the uncertainties due to the aforementioned systematic shifts as $<.001$ Hz (collision); <2 Hz (magnetic field); $<.001$ Hz (electric field); <1 Hz (doppler); $<.001$ Hz (black body radiation).

The Ramsey technique of separated pulses inside the same microwave cavity was also used to measure the transition frequencies as seen in Fig. 5 with a resolution comparable to the reported Rabi measurements. However, because the molecular pulses are extremely monoenergetic, minimal gain was observed in the recovered signal-to-noise ratio. This technique will, of course, be critical for any future molecular fountain clock. The molecular clock could enjoy reduced systematic shifts, such as the magnetic field insensitive transitions demonstrated in this work. It will be most interesting to compare an atomic clock against a molecular one, which depends differently on the fundamental constants. Specifically, the mass dependence of rovibrational transitions in molecules may lead to high resolution studies of the strong interaction.

In summary, microwave spectroscopy was performed on slow, cold molecular pulses produced by a Stark decelerator resulting in the most precise measurement of the OH

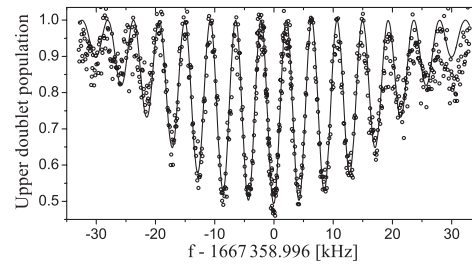


FIG. 5. Ramsey spectroscopy for the $2 \rightarrow 2$ transition with 0.2 ms pulse separation time.

$\Delta F = 0$, Λ -doublet transitions. These results along with appropriate astrophysical measurements of OH megamasers can be used to produce constraints on $\Delta\alpha/\alpha$ with a sensitivity of 1 ppm over the last $\sim 10^{10}$ yr. With continued improvement of the astrophysical measurement of the OH transitions through longer data collection and/or discoveries of new sources, measurement of this molecular system will provide an important and independent constraint on the variation of fundamental constants that date back to the origin of the Universe.

The authors are indebted to Steven Jefferts and John L. Hall for crucial contributions. This work is supported by NSF, NIST, DOE, and the Keck Foundation.

*Electronic address: ehudson@jilau1.colorado.edu

†Electronic address: ye@jila.colorado.edu

- [1] K. Olive and Y. Qian, Phys. Today **57**, No. 10, 40 (2004).
- [2] V. A. Kostelecky, R. Lehnert, and M. J. Perry, Phys. Rev. D **68**, 123511 (2003).
- [3] E. Peik *et al.*, Phys. Rev. Lett. **93**, 170801 (2004).
- [4] J. K. Webb *et al.*, Phys. Rev. Lett. **87**, 091301 (2001).
- [5] R. Quast, D. Reimers, and S. Levshakov, Astron. Astrophys. **415**, L7 (2004).
- [6] P. A. M. Dirac, Nature (London) **139**, 323 (1937).
- [7] J. Darling, Phys. Rev. Lett. **91**, 011301 (2003).
- [8] J. N. Chengalur and N. Kanekar, Phys. Rev. Lett. **91**, 241302 (2003).
- [9] N. Kanekar, J. N. Chengalur, and T. Ghosh, Phys. Rev. Lett. **93**, 051302 (2004).
- [10] J. J. ter Meulen and A. Dymanus, Astrophys. J. **172**, L21 (1972).
- [11] N. Kanekar (private communication).
- [12] H. L. Bethlem, G. Berden, and G. Meijer, Phys. Rev. Lett. **83**, 1558 (1999).
- [13] J. R. Bochinski *et al.*, Phys. Rev. Lett. **91**, 243001 (2003).
- [14] J. van Veldhoven *et al.*, Eur. Phys. J. D **31**, 337 (2004).
- [15] H. E. Radford, Phys. Rev. **122**, 114 (1961).
- [16] H. J. Lewandowski *et al.*, Chem. Phys. Lett. **395**, 53 (2004).
- [17] J. R. Bochinski *et al.*, Phys. Rev. A **70**, 043410 (2004).
- [18] E. R. Hudson *et al.*, Eur. Phys. J. D **31**, 351 (2004).
- [19] A. V. Avdeenko and J. L. Bohn, Phys. Rev. A **66**, 052718 (2002).
- [20] For the TM_{010} mode the electric field is uniform along the cavity axis. However, due to the use of multiple frequencies, we work below the TM_{010} cavity resonance leading to the observed electric field decay.